J|A|C|S
ARTICLES
Published on Web 02/20/2002

Influence of d Orbital Occupation on the Binding of Metal Ions to Adenine

M. T. Rodgers*,† and P. B. Armentrout‡

Contributions from Department of Chemistry, Wayne State University, Detroit, Michigan 48202 and Department of Chemistry, University of Utah, Salt Lake City, Utah 84112

Received May 24, 2001

Abstract: Threshold collision-induced dissociation of M^+(adenine) with xenon is studied using guided ion beam mass spectrometry. M^+ includes all 10 first-row transition metal ions: Sc^+, Ti^+, V^+, Cr^+, Mn^+, Fe^+, Co^+, Ni^+, Cu^+, and Zn^+. For the systems involving the late metal ions, Cr^+ through Cu^+, the primary product corresponds to endothermic loss of the intact adenine molecule, whereas for Zn^+, this process occurs but to form Zn + adenine$^+$. For the complexes to the early metal ions, Sc^+, Ti^+, and V^+, intact ligand loss competes with endothermic elimination of purine and of HCN to form MNH^+ and $M^+(C_4H_4N_4)$, respectively, as the primary ionic products. For Sc^+, loss of ammonia is also a prominent process at low energies. Several minor channels corresponding to formation of $M^+(C_xH_xN_x)$, $x = 1-3$, are also observed for these three systems at elevated energies. The energy-dependent collision-induced dissociation cross sections for M^+(adenine), where $M^+ = V^+$ through Zn^+, are modeled to yield thresholds that are directly related to 0 and 298 K bond dissociation energies for M^+−adenine after accounting for the effects of multiple ion−molecule collisions, kinetic and internal energy distributions of the reactants, and dissociation lifetimes. The measured bond energies are compared to those previously studied for simple nitrogen donor ligands, NH_3 and pyrimidine, and to results for alkali metal cations bound to adenine. Trends in these results and theoretical calculations on Cu^+(adenine) suggest distinct differences in the binding site propensities of adenine to the alkali vs transition metal ions, a consequence of s−dσ hybridization on the latter.

Introduction

Although metal ions are known to participate in biological processes,[1] systematic information on how the identity of the metal influences these functions is difficult to obtain. Certainly, the specific metal identity should be a crucial factor in cases where metal ions play a direct role, such as in oxidation−reduction reactions. In contrast, when metal ions exert a more indirect influence, perhaps by inducing conformational changes, the size and charge of the metal ion may be the most influential aspects. Alternatively, undesired effects can occur when the wrong metals are present, or even essential metals in the wrong concentrations.[2] For example, mispairing of bases in nucleic acids that can occur at high metal ion concentrations could induce misincorporation of an amino acid during protein synthesis. Because different metal ions exhibit different structural effects, the nature of the metal contact in the nucleus can conceivably influence the course of genetic information transfer. For instance, metal ions that preferentially bind to nucleobases may cause more dramatic effects on DNA conformation[3] than those binding to the phosphate and sugar backbone.

In trying to quantitatively assess such interactions in complex biological systems, a potentially useful first step is to measure the intrinsic binding energies of various metal ions to specific parts of biological molecules. Previously, we measured the absolute binding energies of Li^+, Na^+, and K^+ to three nucleobases, uracil, thymine, and adenine.[4] Alkali metal ions, and other "hard" metal ions, have a low tendency to form covalent bonds and are therefore less likely to exhibit strong specificity in their binding sites. Sequential binding energies for such metal ions show gradual decreases in the L_xM^+-L bond energies, consistent with largely electrostatic bonding.[5] Chelating ligands show weaker bond energies that the sum of equivalent independent ligands, a consequence of geometric restrictions on optimizing the orientation of the donor atoms toward the metal ion.,[6−8] In contrast, transition metal ions can form multiple covalent bonds and generally bind much more strongly to simple electron donors[5] (e.g., CO,[9,10] H_2O,[11−14] NH_3,[15] benzene,[16,17] pyridine,[18,19] pyrimidine[18,20]) than the alkali

† Wayne State University.
‡ University of Utah.

(1) Eichhorn, G. L. *Adv. Inorg. Biochem.* **1981**, *3*, 1.
(2) Eichhorn, G. L. In *Inorganic Biochemistry*; Eichhorn, G. L., Ed.; Elsevier: New York, 1973; p 1210.
(3) Shin, Y. A. Eichhorn, G. L. *Biopolymers* **1977,** *16*, 225.
(4) Rodgers, M. T.; Armentrout, P. B. *J. Am. Chem. Soc.* **2000**, *122*, 8548.
(5) Rodgers, M. T.; Armentrout, P. B. *Mass Spectrom. Rev.* **2000**, *19*, 215.
(6) More, M. B.; Ray, D.; Armentrout, P. B. *J. Phys. Chem. A* **1997**, *101*, 831.
(7) More, M. B.; Ray, D.; Armentrout, P. B. *J. Phys. Chem. A* **1997**, *101*, 4254.
(8) Armentrout, P. B. *Int. J. Mass Spectrom.* **1999**, *193*, 227.
(9) Walter, D.; Armentrout, P. B. *Int. J. Mass Spectrom. Ion Process.* **1998**, *175*, 93.
(10) Armentrout, P. B.; Kickel, B. L. In *Organometallic Ion Chemistry*; Freiser, B. S., Ed.; Kluwer: Dordrecht, 1996; pp 1−45.
(11) Armentrout, P. B. *Acc. Chem. Res.* **1995**, *28*, 430.
(12) Dalleska, N. F.; Tjelta, B. L.; Armentrout, P. B. *J. Phys. Chem.* **1994**, *98*, 4191.
(13) Dalleska, N. F.; Honma, K.; Sunderlin, L. S.; Armentrout, P. B. *J. Am. Chem. Soc.* **1994**, *116*, 3519.
(14) Rodgers, M. T.; Armentrout, P. B. *J. Phys. Chem. A* **1997**, *101*, 1238.

10.1021/ja011278+ CCC: $22.00

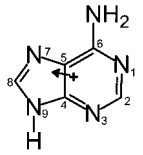

adenine
2.54 D
13.10 Å^3

Figure 1. Structure of adenine. Properly scaled dipole moment in Debye is shown as an arrow (+ indicates the positive end of the dipole). Value listed is taken from theoretical calculations performed in Rodgers and Armentrout.[4] The measured molecular polarizability in Å^3 as cited in Miller.[23]

metal ions. Here, sequential bond energies of ligation can show complex patterns that depend strongly on the d orbital occupation. For many transition metal ions, a most striking observation is that the second ligand can bind as strongly, or in some cases more strongly, than the first ligand, a consequence of s−dσ hybridization.[21] However, this hybridization has a very strong preference for ligation at 180°,[5] such that chelating ligands are under strong geometric constraints.[22] Consequently, chelation may not be as favorable for transition metal ions as for alkali and other "hard" metal ions. In this work, we investigate whether these conclusions hold true for more complex species, in this case, the nucleic acid base, adenine, which has both monodentate (N3) and bidentate (N7−NH_2 and N1−NH_2) binding sites. The structure of adenine is shown in Figure 1 along with a calculated dipole moment[4] and measured polarizability.[23]

In recent work, we have developed methods to allow the application of quantitative threshold collision-induced dissociation (CID) methods to obtain accurate thermodynamic information on increasingly large systems.[4,17−20,24−31] One of the driving forces behind these developments is our interest in applying such techniques to large systems such as those of biological relevance. In the present study, we use guided ion beam mass spectrometry to collisionally excite complexes of M^+ bound to adenine, where $M^+ = Sc^+$, Ti^+, V^+, Cr^+, Mn^+, Fe^+, Co^+, Ni^+, Cu^+, and Zn^+. Kinetic energy-dependent cross sections for the CID processes are analyzed using methods developed previously.[25] The analysis explicitly includes the effects of the internal and translational energy distributions of the reactants, multiple collisions, and the lifetime for dissociation. We derive M^+−adenine bond dissociation energies (BDEs) for all of the complexes but those for which $M^+ = Sc^+$ and Ti^+, and compare these results to previous experimental results obtained for other N-donor molecules bound to M^+, and to the results for alkali metal cations bound to adenine.

In biological systems, alkali cations are found exclusively as the +1 charge state. In contrast, transition metal ions appear in multiple oxidation states which include the +1 charge state for copper, cobalt, and nickel.[32] Further, free metal ions are not important reagents in biological systems; instead they appear in a complex molecular scaffolding that orients ligands to stabilize the metal ions, satisfy their electron deficiency, and permit them to undergo selective chemistry. However, in thinking about the thermodynamics of such species, it should be realized that a formal oxidation state is not equivalent to the real electron deficiency, precisely because the metal ions exist in a solvated or ligated environment where electron density is donated to the metal ion. Indeed, direct measurements of ligand binding affinities to multiply charged bare metal ions would be truly irrelevant to biological function because the increased electron deficiency would cause these metal ions to be much more reactive than when they are present in partially solvated or ligated environments. Therefore, the intrinsic bond energies and reactivities measured here for the +1 oxidation states may be useful analogues of the binding and reactivity of partially solvated M^{2+} or M^{3+} species, where the latter would be difficult to measure directly. Further, such intrinsic bond energies can be combined with solvation energies or the binding energies to other constituents of the biological system to allow a quantitative assessment of the competition among various possible binding sites. In addition, trends in the d orbital occupation, such as those explored in this work, should be largely independent of the charge and can provide insight into details of the binding mechanisms that should be useful in understanding a variety of real chemical environments. Finally, such gas-phase thermochemistry can provide benchmarks for comparison to theory, which may then be used with more confidence on increasingly complex systems. Overall, the measurements described herein can be viewed as providing a useful "thermodynamic vocabulary" for thinking quantitatively about metal ion interactions with biological molecules.

Experimental Section

General Procedures. Cross sections for collision-induced dissociation of M^+(adenine), where $M^+ = Sc^+$, Ti^+, V^+, Cr^+, Mn^+, Fe^+, Co^+, Ni^+, Cu^+, and Zn^+, are measured using one of two guided ion beam tandem mass spectrometers that have been described in detail previously.[30,33] The M^+(adenine) complexes are generated as described below. In both instruments, the ions are extracted from the source, accelerated, and focused into a magnetic sector momentum analyzer for mass analysis. Mass-selected ions are decelerated to a desired kinetic energy and focused into an octopole ion guide, which traps the ions in the radial direction.[34] The octopole passes through a static gas cell containing xenon, used as the collision gas for reasons described elsewhere.[35−37] Low gas pressures in the cell (typically 0.05−0.20 mTorr) are used to ensure that multiple ion−molecule collisions are improbable. Product and unreacted reactant ions drift to the end of the octopole where they are focused into a quadrupole mass filter for mass

(15) Walter, D.; Armentrout, P. B. *J. Am. Chem. Soc.* **1998**, *120*, 3176.
(16) Meyer, F.; Khan, F. A.; Armentrout, P. B. *J. Am. Chem. Soc.* **1995**, *117*, 9740.
(17) Amicangelo, J.; Armentrout, P. B. *J. Phys. Chem. A.* **2000**, *104*, 11420.
(18) Amunugama, R.; Rodgers, M. T. *Int. J. Mass Spectrom.* **2000**, *195/196*, 439.
(19) Rodgers, M. T.; Stanley, J. R.; Amunugama, R. *J. Am. Chem. Soc.* **2000**, *122*, 10969.
(20) Amunugama, R.; Rodgers, M. T. *J. Phys. Chem. A* **2001**, *105*, 9883
(21) Bauschlicher, C. W.; Langhoff, S. R.; Partridge, H. *J. Chem. Phys.* **1991**, *94*, 2068.
(22) Koizumi, H.; Armentrout, P. B. *J. Am. Soc. Mass Spectrom.* **2001**, *12*, 480.
(23) As cited in Miller, K. J. *J. Am. Chem. Soc.* **1990**, *112*, 8533, however, the reference provided therein does not actually contain the listed values.
(24) Rodgers, M. T.; Armentrout, P. B. *J. Phys. Chem. A* **1997**, *101*, 2614.
(25) Rodgers, M. T.; Ervin, K. M.; Armentrout, P. B. *J. Chem. Phys.* **1997**, *106*, 4499.
(26) Rodgers, M. T.; Armentrout, P. B. *J. Chem. Phys.* **1998**, *109*, 1787.
(27) Rodgers, M. T.; Armentrout, P. B. *Int. J. Mass Spectrom.* **1999**, *185/186/187*, 359.
(28) Rodgers, M. T.; Armentrout, P. B. *J. Phys. Chem. A* **1999**, *103*, 4955.
(29) Armentrout, P. B.; Rodgers, M. T. *J. Phys. Chem. A* **2000**, *104*, 2238.
(30) Rodgers, M. T. *J. Phys. Chem. A* **2001**, *105*, 2374.
(31) Rodgers, M. T. *J. Phys. Chem. A* **2001**, *105*, 8145.
(32) Cowan, J. A. *Inorganic Biochemistry: An Introduction*; VCH: New York, 1993.
(33) Ervin, K. M. Armentrout, P. B. *J. Chem. Phys.* **1985**, *83*, 166.
(34) Teloy, E.; Gerlich, D. *Chem. Phys.* **1974**, *4*, 417. Gerlich, D. Diplomarbeit, University of Freiburg, Federal Republic of Germany, 1971. Gerlich, D. State-Selected and State-to-State Ion−Molecule Reaction Dynamics, Part I, Experiment. In *Advances in Chemical Physics*; Ng, C.-Y.; Baer, M., Eds.; Wiley: New York, 1992; Vol. 82, p 1.

Table 1. Enthalpies of Metal Ion Binding to Adenine at 0 K in kJ/mol

			theory									
	experimental		B3LYP				MP2			MPW1PW91		
complex	TCID[a]	literature[b]	D_e[c]	D_e[d]	D_0[e]	$D_{0,BSSE}$[f]	D_e[g]	D_0[e]	$D_{0,BSSE}$[f]	D_e[h]	D_0[e]	$D_{0,BSSE}$[f]
Li^+N7(adenine)	226.1 (6.1)	210 (20)	216.5	216.8	206.8	204.9	218.6	208.3	199.8	212.6	202.4	200.9
Na^+N7(adenine)	139.6 (4.2)	160 (25)	141.1	142.1	135.8	132.2	144.7	138.0	128.6	136.5	130.0	127.5
K^+N7(adenine)	95.1 (3.2)	105 (11)	81.6	82.0	77.5	76.3	93.5	88.3	82.9	80.7	76.1	75.1
Cu^+N7(adenine)	294.3 (10.6)		273.5	274.9	266.6	262.9	294.8	286.4	267.2	272.8	264.3	261.0
Cu^+N3(adenine)			271.1	272.9	266.5	264.1	270.8	264.4	250.0	265.2	258.7	256.5
Cu^+N1(adenine)			253.7	254.8	247.9	244.8	266.3	259.4	242.5	252.8	245.9	243.0

[a] Threshold collision-induced dissociation. Results from Rodgers and Armentrout[4] except for Cu^+ from the present study. [b] Values, as adjusted in Rodgers and Armentrout,[4] from Cerda, B. A.; Wesdemiotis, C. *J. Am. Chem. Soc.* **1996**, *118*, 11884. [c] Calculated at the B3LYP/6-311+G(2d,2p) level of theory using B3LYP/6-31G* optimized geometries. [d] B3LYP/6-311+G(2d,2p) calculation using an extended polarization 3df functions on the metal ion and B3LYP/6-31G* optimized geometries. [e] Including zero point energy corrections with frequencies corresponding to the B3LYP/6-31G* geometries scaled by 0.9804. B3LYP results are those calculated using the extended 3df polarization functions on the metal ion. [f] Also includes basis set superposition error corrections determined at the same level of theory. [g] MP2(full)/6-311+G(2d,2p) calculation using an extended polarization 3df functions on the metal ion and B3LYP/6-31G* optimized geometries. [h] MPW1PW91/6-311+G(2d,2p) calculation using MPW1PW91/6-31G* optimized geometries.

analysis and subsequently detected with a secondary electron scintillation detector and standard pulse counting techniques. Ion intensities are converted to absolute cross sections as described previously.[33] Absolute uncertainties in cross section magnitudes are estimated to be ±20%, which are largely the result of errors in the pressure measurement and the length of the interaction region. Relative uncertainties are approximately ±5%.

Ion kinetic energies in the laboratory frame, E_{lab}, are converted to energies in the center of mass frame, E_{CM}, using the formula $E_{CM} = E_{lab}\, m/(m+M)$, where M and m are the masses of the ionic and neutral reactants, respectively. All energies reported below are in the CM frame unless otherwise noted. The absolute zero and distribution of the ion kinetic energies are determined using the octopole ion guide as a retarding potential analyzer as previously described.[33] The distribution of ion kinetic energies is nearly Gaussian with a fwhm typically between 0.2 and 0.4 eV (lab) for these experiments. The uncertainty in the absolute energy scale is ± 0.05 eV (lab).

Even when the pressure of the reactant neutral is low, it has previously been demonstrated that the effects of multiple collisions can significantly influence the shape of CID cross sections.[13] Because the presence and magnitude of these pressure effects is difficult to predict, we have performed pressure-dependent studies of all cross sections examined here. In the present systems, we observe small cross sections at low energies that have an obvious dependence upon pressure. We attribute this to multiple energizing collisions that lead to an enhanced probability of dissociation below threshold as a result of the longer residence time of these slower moving ions. Data free from pressure effects are obtained by extrapolating to zero reactant pressure, as described previously.[13] Thus, cross sections subjected to analysis are the result of single bimolecular encounters.

Ion Source. The M^+(adenine) complexes are formed in a 1 m long flow tube[30,38] operating at a pressure of 0.7−0.8 Torr with a helium flow rate of 4000−5000 sccm. Metal ions are generated in a continuous dc discharge by argon ion sputtering of a cathode made from the metal of interest, or a tantalum boat containing the metal in the case of Mn. Typical operating conditions of the discharge for transition metal ion production are 0.8−2.8 kV and 5−22 mA in a flow of roughly 10% argon in helium. The M^+(adenine) complexes are formed by associative reactions of the transition metal ion with the neutral adenine molecule, which is introduced into the flow 50 cm downstream from the dc discharge. The vapor pressure of adenine was not sufficient to carry out these experiments without gentle heating and flowing helium over the sample. The flow conditions used in this ion source provide in excess of 10^5 collisions between an ion and the buffer gas, which should thermalize the ions both vibrationally and rotationally. In our analysis of the data, we assume that the ions produced in this source are in their ground electronic states and that the internal energy of the M^+(adenine) complexes is well described by a Maxwell−Boltzmann distribution of rovibrational states at 300 K. Previous work from our laboratories has shown that these assumptions are generally valid.[13,14,35,38−41]

Thermochemical Analysis. The threshold regions of the reaction cross sections are modeled using eq 1,

$$\sigma(E) = \sigma_0 \sum_i g_i (E + E_i - E_0)^n / E \qquad (1)$$

where σ_0 is an energy independent scaling factor, E is the relative translational energy of the reactants, E_0 is the threshold for reaction of the ground electronic and rovibrational state, and n is an adjustable parameter that describes the efficiency of collisional energy transfer.[42] The summation is over the rovibrational states of the reactant ions, i, where E_i is the excitation energy of each state and g_i is the population of those states ($\Sigma g_i = 1$). The populations of excited rovibrational levels are not negligible even at 298 K as a result of the many low-frequency modes present in these ions. The relative reactivity of all rovibrational states, as reflected by σ_0 and n, is assumed to be equivalent.

To obtain vibrational frequencies for the neutral and metalated adenine, we scaled frequencies obtained from ab initio calculations, performed using *Gaussian 98*,[43] at the MP2(full)/6-31G* level on Na^+−(adenine) where the metal is bound at the N7 site.[4] The frequencies for the adenine ligand were scaled by a factor of 0.9646,[44] and the calculated metal−ligand frequencies were adjusted to values appropriate for the transition metal systems using a reduced Morse potential procedure outlined elsewhere.[15] The scaled vibrational frequencies thus obtained were assumed identical for all metal systems examined here and are available as Supporting Information, listed in Table 1S. To

(35) Dalleska, N. F.; Honma, K.; Armentrout, P. B. *J. Am. Chem. Soc.* **1993**, *115*, 12125.
(36) Aristov, N.; Armentrout, P. B. *J. Phys. Chem.* **1986**, *90*, 5135.
(37) Hales, D. A.; Armentrout, P. B. *J. Cluster Sci.* **1990**, *1*, 127.
(38) Schultz, R. H.; Armentrout, P. B. *J. Chem. Phys.* **1992**, *96*, 1046.
(39) Schultz, R. H.; Crellin, K. C.; Armentrout, P. B. *J. Am. Chem. Soc.* **1992**, *113*, 8590.
(40) Khan, F. A.; Clemmer, D. E.; Schultz, R. H.; Armentrout, P. B. *J. Phys. Chem.* **1993**, *97*, 7978.
(41) Fisher, E. R.; Kickel, B. L.; Armentrout, P. B. *J. Phys. Chem.* **1993**, *97*, 10204.
(42) Muntean, F.; Armentrout, P. B. *J. Chem. Phys.* **2001**, *115*, 1213.
(43) Frisch, M. J.; Trucks, G. W.; Schlegel, H. B.; Scuseria, G. E.; Robb, M. A.; Cheeseman, J. R.; Zakrzewski, V. G.; Montgomery, J. A., Jr.; Stratmann, R. E.; Burant, J. C.; Dapprich, S.; Millam, J. M.; Daniels, A. D.; Kudin, K. N.; Strain, M. C.; Farkas, O.; Tomasi, J.; Barone, V.; Cossi, M.; Cammi, R.; Mennucci, B.; Pomelli, C.; Adamo, C.; Clifford, S.; Ochterski, J.; Petersson, G. A.; Ayala, P. Y.; Cui, Q.; Morokuma, K.; Malick, D. K.; Rabuck, A. D.; Raghavachari, K.; Foresman, J. B.; Cioslowski, J.; Ortiz, J. V.; Stefanov, B. B.; Liu, G.; Liashenko, A.; Piskorz, P.; Komaromi, I.; Gomperts, R.; Martin, R. L.; Fox, D. J.; Keith, T.; Al-Laham, M. A.; Peng, C. Y.; Nanayakkara, A.; Gonzalez, C. Challacombe, M.; Gill, P. M. W.; Johnson, B.; Chen, W. Wong, M. W.; Andres, J. L.; Gonzales, C.; Head-Gordon, M.; Replogle, E. S.; Pople, J. A. *Gaussian 98*, rev A.9, Gaussian, Inc. Pittsburgh, PA, 1998.
(44) Foresman, J. B.; Frisch, Æ. *Exploring Chemistry with Electronic Structure Methods*, 2nd ed.; Gaussian: Pittsburgh, 1996.

Table 2. Fitting Parameters of Eq 1, Threshold Dissociation Energies at 0 K, and Entropies of Activation at 1000 K of M^+(Adenine)[a]

reactant ion	product ion	σ_0[b]	n[b]	E_0[c](eV)	$E_{0(PSL)}$ (eV)	kinetic shift (eV)	$\Delta S^{\ddagger}$(PSL) (J mol^{-1} K^{-1})
Ti^+(adenine)	Ti^+	0.16 (0.03)	1.6 (0.1)	≤ 4.36 (0.19)	≤ 3.52 (0.15)	0.84	68 (5)
Ti^+(adenine)	$TiNH^+$	6.2 (1.5)[c]	1.8 (0.2)[c]	≤ 3.45 (0.08)			
V^+(adenine)	V^+	5.7 (1.0)	1.5 (0.2)	≤ 3.45 (0.11)	≤ 2.75 (0.11)	0.70	70 (5)
V^+(adenine)	VNH^+	5.0 (1.0)[c]	1.5 (0.2)[c]	≤ 2.95 (0.12)			
Cr^+(adenine)	Cr^+	14.6 (0.6)	1.1 (0.1)	2.88 (0.04)	2.39 (0.08)	0.49	71 (5)
Mn^+(adenine)	Mn^+	15.4 (0.9)	1.1 (0.1)	2.66 (0.09)	2.24 (0.08)	0.42	72 (5)
Fe^+(adenine)	Fe^+	8.8 (0.8)	1.4 (0.1)	3.35 (0.06)	2.69 (0.09)	0.66	71 (5)
Co^+(adenine)	Co^+	7.1 (0.6)	1.3 (0.1)	3.93 (0.08)	3.04 (0.11)	0.89	71 (5)
Ni^+(adenine)	Ni^+	3.5 (0.6)	1.8 (0.1)	3.99 (0.05)	3.08 (0.10)	0.91	71 (5)
Cu^+(adenine)	Cu^+	6.1 (0.4)	1.3 (0.1)	3.92 (0.06)	3.04 (0.11)	0.88	72 (5)
Cu^+(adenine)[d]	Cu^+	6.1 (0.4)	1.3 (0.1)	3.92 (0.06)	3.09 (0.11)	0.83	67 (5)
Cu^+(adenine)[e]	Cu^+	6.3 (0.4)	1.3 (0.1)	3.94 (0.06)	2.98 (0.11)	0.96	46 (5)
Zn^+(adenine)	adenine$^+$	34.4 (1.1)	1.3 (0.1)	1.71 (0.04)	1.54 (0.05)	0.17	51 (6)

[a] Uncertainties are listed in parentheses. Analyses performed using frequencies scaled from Na^+N7(adenine), Table 1S, except as noted. [b] Average values for loose PSL transition state, except for MNH^+ products. [c] No RRKM analysis. [d] Analyses performed using frequencies calculated for Cu^+N7(adenine) at the B3LYP/6-31G* level, Table 1S. [e] Analyses performed using frequencies calculated for Cu^+N3(adenine) at the B3LYP/6-31G* level, Table 1S.

model the dissociation of Zn^+(adenine), we also required the frequencies for adenine$^+$, which were calculated at a B3LYP/6-31G* level and scaled by 0.9804.[44] These values are also listed in Table 1S. Rotational constants for the M^+(adenine) complexes are assumed to equal those calculated at the MP2(full)/6-31G* level for the K^+(adenine) complex,[4] because K^+ has a mass comparable to the transition metals studied here. These are listed in Table 2S.

The advantage of this procedure for determining molecular constants is that calculations on very simple systems can be used to evaluate these parameters for systems that are not easily amenable to theoretical treatment. To test this assumption, we have performed theoretical calculations on Cu^+(adenine) in several conformations, as described below. Frequencies obtained in this fashion were scaled by a factor of 0.9804[44] and are also listed in Table 1S. Table 2S contains the rotational constants calculated directly. The mean deviation between the frequencies scaled from Na^+(adenine) and those calculated directly for the Cu^+N7(adenine) complex is 2.3 ± 8.9%, such that our use of 10% uncertainties in the frequencies (see below) easily encompasses variations among the various sets of molecular parameters. The main difference between these sets of vibrations is that there is no imaginary frequency associated with NH_2 rotation in the directly calculated frequencies for Cu^+(adenine), in contrast to those for Na^+(adenine). Hence, there is a low-frequency vibration that replaces the 1-D rotor used in the frequencies scaled from the latter complex. As described below, we examine the sensitivity of the fitting results to the choice of the molecular parameters in our analysis of the data.

The Beyer−Swinehart algorithm[45] is used to evaluate the density of the rovibrational states and the relative populations, g_i, are calculated by an appropriate Maxwell−Boltzmann distribution at the 298 K temperature appropriate for the reactants. The average vibrational energy at 298 K of the metal ion-bound adenine is also given in Table 1S. We have estimated the sensitivity of our analysis to the deviations from the true frequencies by scaling the calculated frequencies to encompass the range of average scaling factors needed to bring calculated frequencies into agreement with experimentally determined frequencies found by Pople et al.[46] Thus, the originally calculated and appropriately scaled vibrational frequencies were increased and decreased by 10% for ligand modes and by 20% for the three metal−ligand modes. The corresponding change in the average vibrational energy is taken to be an estimate of one standard deviation of the uncertainty in vibrational energy (Table 1S) and is included in the uncertainties listed with the E_0 values.

We also consider the possibility that collisionally activated complex ions do not dissociate on the time scale of our experiment (approximately 10^{-4} s) by including statistical theories for unimolecular dissociation, specifically Rice−Ramsperger−Kassel−Marcus (RRKM) theory, into eq 1 as described in detail elsewhere.[25,40] This requires sets of rovibrational frequencies appropriate for the energized molecules and the transition states (TSs) leading to dissociation. The former sets are given in Tables 1S and 2S, whereas we assume that the TSs are loose and product-like because the interaction between the metal ion and the adenine ligand (or the zinc atom and the adenine ion) is largely electrostatic. In this case, the TS vibrations used, which are also found in Table 1S, are the frequencies corresponding to the adenine (or adenine$^+$) product. The transitional frequencies, those that become rotations of the completely dissociated products, are treated as rotors, a treatment that corresponds to a phase space limit (PSL) and is described in detail elsewhere.[25] For the M^+(adenine) complexes, the two transitional mode rotors have rotational constants equal to those of the neutral adenine product with axes perpendicular to the reaction coordinate. These are listed in Table 2S. The external rotations of the energized molecule and TS are also included in the modeling of the CID data. The external rotational constants of the TS are determined by assuming that the TS occurs at the centrifugal barrier for interaction of M^+ with the neutral adenine ligand (or Zn with adenine$^+$), calculated variationally as outlined elsewhere.[25] The 2-D external rotations are treated adiabatically but with centrifugal effects included, consistent with the discussion of Waage and Rabinovitch.[47] In the present work, the adiabatic 2-D rotational energy is treated using a statistical distribution with an average rotational energy, as described in detail elsewhere.[25] Analyses with an explicit summation over the possible values of the rotational quantum number were also tested and found to provide nearly identical results.

The model represented by eq 1 is expected to be appropriate for translationally driven reactions[48] and has been found to reproduce reaction cross sections well in a number of previous studies of both atom−diatom and polyatomic reactions,[49,50] including CID processes.[4−19,24−31,35,39,40] In addition, we have recently demonstrated that the cross section form given in eq 1 is consistent with direct measurements of the energy transferred in collisions between $Cr(CO)_6^+$ with Xe,[42] a result that provides increased confidence in the use of this model to obtain accurate thermodynamic information from CID thresholds. The model of eq 1 is convoluted with the kinetic energy distributions of both reactants, and a nonlinear least-squares analysis of the data is performed to give optimized values for the parameters σ_0, E_0, and n. The error associated with the measurement of E_0, reported as one standard deviation, is estimated from the range of threshold values determined for different zero-pressure extrapolated data sets,

(45) Beyer, T. S.; Swinehart, D. F. *Comm. Assoc. Comput. Machines* **1973**, *16*, 379. Stein, S. E.; Rabinovitch, B. S. *J. Chem. Phys.* **1973**, *58*, 2438. *Chem. Phys. Lett.* **1977**, *49*, 183.
(46) Pople, J. A.; Schlegel, H. B.; Raghavachari, K.; DeFrees, D. J.; Binkley, J. F.; Frisch, M. J.; Whitesides, R. F.; Hout, R. F.; Hehre, W. J. *Int. J. Quantum Chem. Symp.* **1981**, *15* 269. DeFrees, D. J.; McLean, A. D. *J. Chem. Phys.* **1985**, *82*, 333.
(47) Waage, E. V.; Rabinovitch, B. S. *Chem. Rev.* **1970**, *70*, 377.
(48) Chesnavich, W. J.; Bowers, M. T. *J. Phys. Chem.* **1979**, *83*, 900.
(49) Armentrout, P. B., In *Advances in Gas-Phase Ion Chemistry*; Adams, N. G., Babcock, L. M. Eds.; JAI; Greenwich, 1992; Vol. 1, pp 83−119.
(50) See, for example: Sunderlin, L. S.; Armentrout, P. B. *Int. J. Mass Spectrom. Ion Processes* **1989**, *94*, 149.

variations associated with uncertainties in the vibrational frequencies, and the error in the absolute energy scale, 0.05 eV (lab). For analyses that include the RRKM lifetime effect, the uncertainties in the reported E_0 values also include the effects of increasing and decreasing the time assumed available for dissociation by a factor of 2.

Equation 1 explicitly includes the internal energy of the ion, E_i. All energy available is treated statistically, which should be a reasonable assumption because the internal (rotational and vibrational) energy of the reactants is redistributed throughout the ion upon impact with the collision gas. The threshold for dissociation is by definition the minimum energy required leading to dissociation and thus corresponds to formation of products with no internal excitation. The assumption that products formed at threshold have an internal temperature of 0 K has been tested for several systems.[13,14,24,35,36,39,40] It has also been shown that treating all energy of the ion (vibrational, rotational, and translational) as capable of coupling into the dissociation coordinate leads to reasonable thermochemistry. The threshold energies for dissociation reactions determined by analysis with eq 1 are converted to 0 K bond energies by assuming that E_0 represents the energy difference between reactants and products at 0 K.[51] This assumption requires that there are no activation barriers in excess of the endothermicity of dissociation. This is generally true for ion−molecule reactions[49] and should be valid for the heterolytic bond fission reactions examined here.[52]

Theoretical Calculations. To obtain model structures, vibrational frequencies, and energetics for the neutral and metalated (with Li^+, Na^+, K^+, and Cu^+) adenine molecule, density functional calculations were performed using *Gaussian 98*.[43] Calculations on the open-shell transition metal ion (Sc^+, Ti^+, V^+, Cr^+, Mn^+, Fe^+, Co^+, Ni^+, and Zn^+) complexes are sufficiently complicated[19,20] that they were not pursued in this work. Geometry optimizations were performed at the B3LYP/6-31G* level. Vibrational analyses of the geometry-optimized structures were performed at this same level to determine the vibrational frequencies and rotational constants of the molecules. When used to model the data or to calculate thermal energy corrections, the B3LYP/6-31G* vibrational frequencies were scaled by a factor of 0.9804[44] and are listed in Table 1S. Table 2S lists the rotational constants for the ground state conformations.

Single point energy calculations were performed at the B3LYP/6-311+G(2d,2p) and MP2(full)/6-311+G(2d,2p) levels using the B3LYP/6-31G* geometries. We also performed B3LYP/6-311+G(2d,2p) single point calculations using extended 3df polarization functions on copper. Recently, it has been suggested that the MPW1PW91 functional may be a better choice to accurately describe some transition metal systems,[53] hence, we also performed MPW1PW91/6-311+G(2d,2p)//MPW1PW91/6-31G* calculations on these four complexes. This uses a one parameter functional with a modified Perdew−Wang exchange functional and the Perdew−Wang 91 correlation functional.[54] In all cases, accurate bond dissociation energies were obtained by applying zero point energy (ZPE) corrections and subtracting basis set superposition errors (BSSE) from the computed dissociation energies in the full counterpoise approximation,[55,56] as in several other recent papers on metalated complexes.[57−59] The ZPE corrections range from 4.5 kJ/mol for the K^+ complex and increase with the charge density of the cation to 6.3 kJ/mol for Na^+, 6.8−8.3 kJ/mol for Cu^+, and 10.0 kJ/mol for the Li^+ complex. The BSSE corrections for the B3LYP calculations (which used the 3df polarization set on copper) were small, and range from 1.2 kJ/mol for the K^+ complex to 3.6 kJ/mol for Na^+, 2.4−3.7 kJ/mol for Cu^+, and 1.9 kJ/mol for the Li^+ complex. Similar values are obtained for the MPW1PW91 calculations: 1.0, 2.5, 2.2−3.3, and 1.5 kJ/mol, respectively. For the MP2(full)/6-311+G(2d,2p)//B3LYP/6-31G* single point calculations, the BSSE corrections for Cu^+ are larger and range from 14.4 to 19.3 kJ/mol. The relative size of the BSSE corrections for B3LYP vs MP2 calculations are consistent with previous work on a variety of Na^+(ligand) complexes[29] and with comparisons to our previous MP2(full)/6-311+G(2d,2p)//MP2(full)/6-31G* calculations on the alkali cation complexes of adenine bound at the N7, N3, and N1 sites, which had BSSE corrections of 4.2−5.4 for K^+, 7.2−9.4 for Na^+, and 6.3−8.5 for Li^+.[4]

We carefully considered various possible binding sites, N1, N3, and N7, on the adenine ligand for Cu^+. In an earlier study,[4] stable minima were found for all of the alkali metal ions at each of these binding sites. Complexes in which the metal ion binds out of the plane of the molecule to the π-electrons were investigated in that study for Li^+ and found to be much less stable than the in-plane complexes. Thus calculations on comparable π-complexes were not pursued here.

In a few of the systems, one imaginary frequency was obtained for the optimized structures. In free adenine, this was the NH_2 umbrella motion, i.e., motion of the two amino hydrogen atoms out of the plane of the molecule. This vibration is particularly low because the amino group in adenine is planar so that π-electron delocalization can occur. Imaginary frequencies were also obtained for Na^+ and K^+ complexes with adenine bound at the N7 site. In these cases, the motion in which the amino group rotates about the C−N bond is found to be imaginary. No imaginary frequencies occur in the corresponding Li^+ complex as a result of the much stronger binding interaction in this system. Likewise, no imaginary frequencies were found in any of the Cu^+ complexes, even when Cu^+ binds at the N3 site, remote to the amino group. This is somewhat surprising because the NH_2 group is again planar as in neutral adenine. Apparently, metal ion binding at N3 induces sufficient charge transfer to enhance the double bond character of the C−NH_2 bond, see below. In all cases that do have imaginary frequencies, we reassigned them as 1-D rotors with a rotational constant equivalent to the appropriate NH_2 motion. (In assigning these constants, we found that explicit consideration of the remainder of the adenine molecule produced insignificant changes in the values assigned.) The appropriate rotational constants, listed in Table 2S, are different in adenine and the complex systems.

Results

Cross Sections for Collision-Induced Dissociation. Experimental cross sections were obtained for the interaction of Xe with 10 M^+(adenine) complexes, where $M^+ = Sc^+$, Ti^+, V^+, Cr^+, Mn^+, Fe^+, Co^+, Ni^+, Cu^+, and Zn^+. Figure 2 shows representative data for the Sc^+(adenine), Ti^+(adenine), V^+-(adenine), Cu^+(adenine), and Zn^+(adenine) complexes. The other M^+(adenine) complexes show relative behavior similar to that of Cu^+(adenine) and are included in the Supporting Information as Figures 1S. The most favorable process for most complexes is the loss of the intact adenine molecule in the CID reactions 2.

$$M^+(\text{adenine}) + Xe \rightarrow M^+ + \text{adenine} + Xe \qquad (2)$$

The magnitudes of the cross sections for these processes are similar with maxima that vary between 5 and 9 Å^2 for $M^+ = V^+ - Cu^+$.

For Zn^+(adenine), the same dissociation process occurs but the relative ionization energies of the fragments, IE(Zn) = 9.394 eV[60] and IE(adenine) = 8.46 ± 0.05 eV,,[61,6263] are such that

(51) See for example, Figure 1 in Dalleska et al.[35]
(52) Armentrout, P. B.; Simons, J. *J. Am. Chem. Soc.* **1992**, *114*, 8627.
(53) de Oliveira, G.; Martin, J. M. L.; de Proft, F.; Geerlings, P. *Phys. Rev. A* **1999**, *60*, 1034.
(54) Adamo, C.; Barone, V. *J. Chem. Phys.* **1998**, *108*, 664.
(55) Boys, S. F.; Bernardi. R. *Mol. Phys.* **1979**, *19*, 553.
(56) van Duijneveldt, F. B.; van Duijneveldt-van de Rijdt, J. G. C. M.; van Lenthe, J. H. *Chem. Rev.* **1994**, *94*, 1873.
(57) Hill, S. E.; Glendening, E. D.; Feller, D. *J. Phys. Chem. A* **1997**, *101*, 6125.
(58) Hill, S. E.; Feller. D.; Glendening, E. D. *J. Phys. Chem. A* **1998**, *102*, 3813.
(59) Nicholas, J. B.; Hay, B. P.; Dixon, D. A. *J. Phys. Chem.* **1999**, *103*, 1394.
(60) Moore, C. E. Nat. Bur. Stand., NSRDS−NBS-35, Vol. I, 1971; p 1.
(61) Hush, N. S.; Cheung, A. S. *Chem. Phys. Lett.* **1975**, *34*, 11.

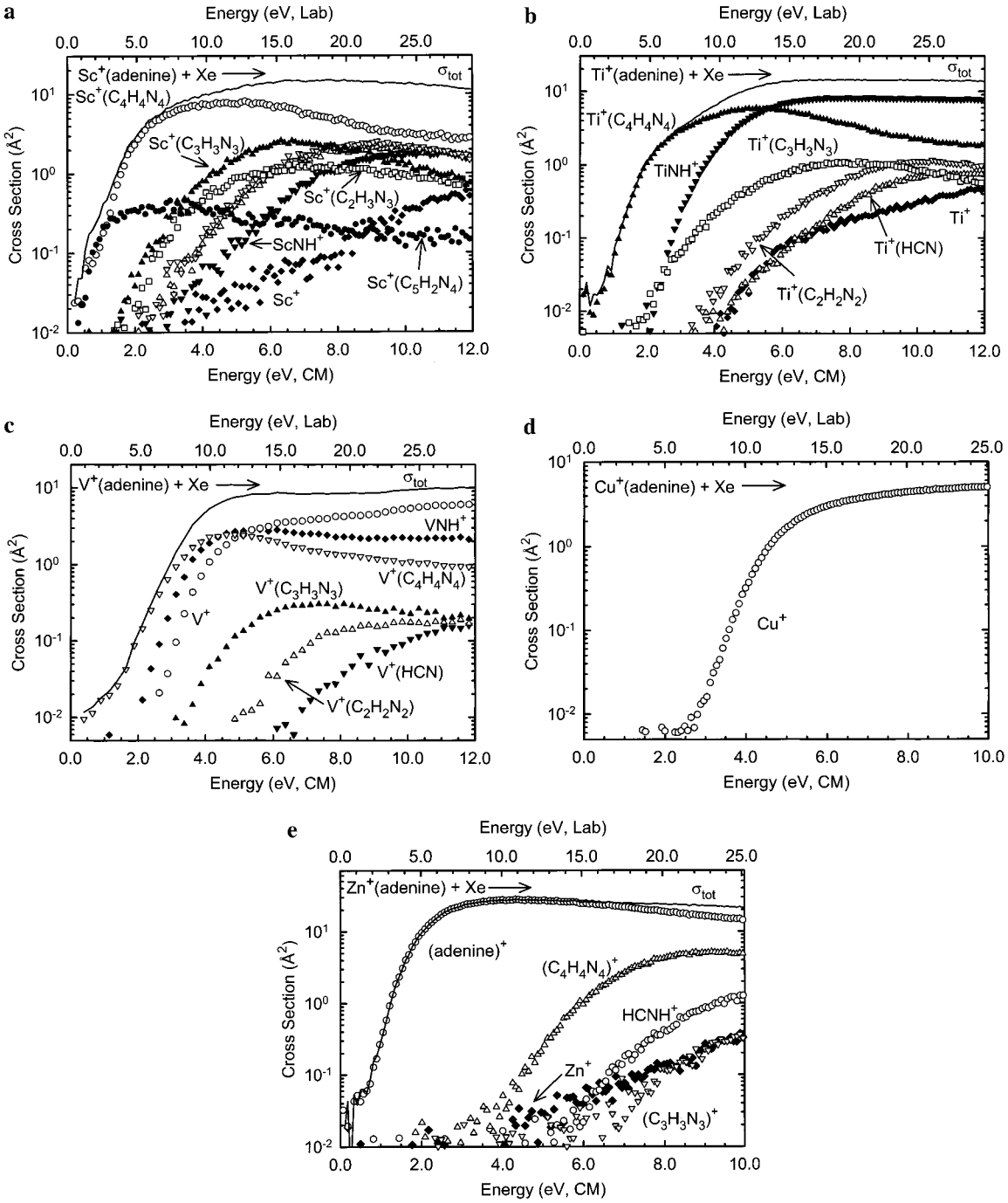

Figure 2. Cross sections for collision-induced dissociation of the M^+(adenine) complex, where $M^+ = Sc^+$ (part a), Ti^+ (part b), V^+ (part c), Cu^+ (part d), and Zn^+ (part e), with Xe as a function of kinetic energy in the center-of-mass frame (lower *x*-axis) and the laboratory frame (upper *x*-axis). Data are shown for Xe pressures of ~0.20 mTorr. In part a, $Sc^+(C_2H_2N_2)$ is represented by ▽ and $Sc^+(CH_2N_2)$ by △.

the ionic product is now the ligand, reaction 3.

$$Zn^+(\text{adenine}) + Xe \rightarrow Zn + \text{adenine}^+ + Xe \qquad (3)$$

Small amounts of Zn^+ are formed at elevated energies, but this channel is clearly suppressed by competition with reaction 3. Subsequent decomposition of the primary adenine$^+$ product by sequential loss of one and two HCN molecules is also observed along with $HCNH^+$ at elevated energies in this system.

The chemistry observed for the early transition metal systems, Sc^+(adenine), Ti^+(adenine), and V^+(adenine), shows much greater complexity, Figures 2a−c. Several other products are observed and include species corresponding to reactions 4−9.

$$M^+(C_5H_5N_5) + Xe \rightarrow MNH^+ + C_5H_4N_4 + Xe \qquad (4)$$

$$\rightarrow M^+(HCN) + [C_4H_4N_4] + Xe \qquad (5)$$

$$\rightarrow M^+(C_2H_2N_2) + [C_3H_3N_3] + Xe \qquad (6)$$

$$\rightarrow M^+(C_3H_3N_3) + [C_2H_2N_2] + Xe \qquad (7)$$

$$\rightarrow M^+(C_4H_4N_4) + HCN + Xe \qquad (8)$$

$$\rightarrow M^+(C_5H_2N_4) + NH_3 + Xe \qquad (9)$$

Table 3. Enthalpies and Free Energies of Metal Ion Binding to Adenine at 298 K in kJ/mol[a]

system	ΔH_0[b]	$\Delta H_{298} - \Delta H_0$[c]	ΔH_{298}	$T\Delta S_{298}$[c]	ΔG_{298}
Ti^+(adenine)	≤339.6 (14.5)	3.8 (3.1)	≤343.4 (14.8)	39.4 (4.7)	≤304.0 (15.5)
V^+(adenine)	≤265.5 (10.6)	3.8 (3.1)	≤269.3 (11.0)	39.5 (4.7)	≤229.8 (12.0)
Cr^+(adenine)	230.6 (7.5)	3.8 (3.1)	234.4 (8.1)	39.6 (4.7)	194.8 (9.4)
Mn^+(adenine)	216.0 (7.4)	3.8 (3.1)	219.8 (8.1)	39.7 (4.7)	180.1 (9.4)
Fe^+(adenine)	259.4 (8.5)	3.8 (3.1)	263.2 (9.0)	39.8 (4.7)	223.4 (10.2)
Co^+(adenine)	293.2 (10.6)	3.8 (3.1)	297.0 (11.0)	39.9 (4.7)	257.1 (12.0)
Ni^+(adenine)	297.5 (9.6)	3.8 (3.1)	301.3 (10.1)	40.1 (4.7)	261.2 (11.1)
Cu^+(adenine)	294.3 (10.6)	3.8 (3.1)	298.1 (11.0)	40.1 (4.7)	258.0 (12.0)
N7	267.2[d]	3.2 (2.2)[e]	270.4	42.3 (4.9)[e]	223.8
N3	250.0[d]	1.6 (1.9)[e]	251.6	37.6 (5.5)[e]	214.0
N1	242.5[d]	2.2 (1.8)[e]	244.7	35.0 (5.4)[e]	209.7
Zn^+(adenine)	≥238.4 (5.6)	3.8 (3.1)	≥242.2 (6.4)	40.1 (4.8)	≥202.1 (8.0)
Zn^+(adenine)[f]	148.3 (4.7)	2.7 (2.0)	151.0 (5.1)	34.2 (4.2)	116.8 (6.6)

[a] Uncertainties are listed in parentheses. [b] Experimental values taken from Table 2, except as noted. [c] Except as noted, values are calculated using vibrational frequencies scaled from Na^+N7(adenine), Table 1S, and rotational constants from K^+N7(adenine), and transitional frequencies appropriately scaled as described in Walter and Armentrout.[15] Uncertainties in these values include the dispersion in values calculated using the molecular constants calculated using B3LYP theory. [d] Theoretical MP2 values taken from Table 1 including ZPE and BSSE corrections. [e] Density functional values from calculations of Cu^+(adenine) at the B3LYP/6-31G* level of theory with all frequencies scaled by 0.9804. [f] These values are for the Zn + adenine$^+$ asymptote.

Sc^+(adenine) alone exhibits reaction 9, a process that is clearly hindered by competition shortly after its threshold. For all three metals, reaction 8 is the dominant low energy process overall, and for $M^+ = V^+$, this is followed at slightly higher energies by reaction 4, and then reaction 2. These three processes must be coupled as the total cross section varies smoothly with kinetic energy and the cross section for reaction 8 declines as reactions 2 and 4 become available. In the Sc^+ and Ti^+ systems, reactions 2 are much less efficient, presumably victims of competition with the other primary channels. In the Sc^+ system, reaction 4 is also suppressed by competition, whereas this process is quite efficient for Ti^+. Reaction 4 almost certainly involves activation of the C6−NH_2 bond followed by reductive elimination of purine, $C_5H_4N_4$, the only reaction pathway except CID in which the aromatic bicyclic ring structure remains intact. This process is feasible as Sc^+, Ti^+, and V^+ are known to exothermically dehydrogenate ammonia,[64,65] again generating MNH^+, in a bimolecular reaction. This exothermic reactivity is consistent with the observation here that the M^+ + adenine product channel, reaction 2, has a higher threshold than reaction 4, although this is difficult to ascertain with certainty in the scandium system. In all three systems, the energy dependence of reaction 7 is potentially consistent with HCN loss from the primary product of reaction 8, i.e., the neutral products in reaction 7 may be two HCN molecules. Likewise, reactions 5 and 6 have energy dependences that are consistent with sequential loss of HCN molecules. Insufficient information is available to discriminate between neutral products that are series of HCN molecules and more complicated molecular species, or to ascertain what structures the $M^+(C_xH_xN_x)$, $x = 2-4$, species might have. We also note that several other products are observed at elevated energies in these three early metal systems. For Sc^+, we also observe $Sc^+(C_2H_3N_3)$ and Sc^+-(CH_2N_2), shown in Figure 2a, and $HCNH^+$ (not shown for clarity, reaches a magnitude of 0.3 Å^2 at 12 eV). In the Ti^+ system, we observe $Ti^+(C_5H_4N_4)$, (not shown for clarity, reaches a magnitude of 0.4 Å^2 at 12 eV); $Ti^+(CH_2N_2)$, (not shown for clarity, reaches a magnitude of 1 Å^2 at 12 eV); and $HCNH^+$ (not shown for clarity, reaches a magnitude of 0.15 Å^2 at 12 eV). $HCNH^+$ is also observed in the Cr^+ system (Fig. S1d).

Theoretical Results. In an earlier study,[4] we investigated the interactions of the alkali metal ions, Li^+, Na^+, and K^+, with adenine at the MP2(full)/6-311+G(2d,2p)//MP2(full)/6-31G* level of theory. Stable conformations were found for all three metal ions at the N1, N3, and N7 sites. In all cases, the alkali metal cation prefers to bind to adenine at the N7 position where there is also a chelation interaction with the amino group. Binding at N1 with chelation to the NH_2 group is only slightly weaker (by 8.0, 4.0, and 0.5 kJ/mol for Li^+, Na^+, and K^+, respectively) than binding at the N7 site, whereas binding at the N3 site is less preferred (by 28.6, 14.6, and 0.9 kJ/mol, respectively) because there is no chelation interaction with the NH_2 group. These comparisons utilize calculated values corrected for ZPE and BSSE. Our present calculations, which utilize the same basis set but B3LYP instead of MP2(full), find geometries of the alkali metal ion bound to adenine at the N7 chelation site that are nearly identical to those found previously.[4] Bond energies (corrected for ZPE and BSSE) are greater in the B3LYP calculations than the MP2 values by 5.1 kJ/mol for Li^+ and 3.6 kJ/mol for Na^+, Table 1. This is consistent with previous comparisons of these two levels of theory made for the bond energies of a variety of Na^+(ligand) complexes.[29] The opposite trend is observed for the K^+ complex where the MP2 bond energy is 6.6 kJ/mol stronger than the B3LYP result. MPW1PW91 results are closer to the MP2 values for Li^+ and Na^+ complexes, differing by only about 1 kJ/mol, whereas the K^+ complex has a MPW1PW91 value close to the B3LYP calculation, Table 1.

In the present work, theoretical structures for neutral adenine and for the complexes of adenine with Cu^+ bound at the N1, N3, and N7 positions were calculated at the B3LYP/6-31G* and MPW1PW91/6-31G* levels. Table 3S gives details of the final B3LYP and MPW1PW91 geometries for each of the Cu^+ bound species. Compared to the B3LYP geometries, MPW1PW91 structures are very similar with bond angles differing by less than 0.3° and bond lengths between heavy atoms systematically shorter by an average of 0.006 Å. B3LYP structures of the three stable conformations of the Cu^+(adenine) complex are shown in Figure 3.[66] As for the alkali cation complexes, binding at the N7 site is favorable for Cu^+ because of the chelation interaction

(62) Peng, S.; Padva, A.; LeBreton, P. R. *Proc. Nat. Acad. Sci. U.S.A.* **1976**, *73*, 2966.
(63) Lin, J. Yu, C.; Peng, S.; Akiyama, I.; Li, K.; Lee, L. K.; LeBreton, P. R. *J. Am. Chem. Soc.* **1980**, *102*, 4627.
(64) Clemmer, D. E.; Sunderlin, L. S.; Armentrout, P. B. *J. Phys. Chem.* **1990**, *94*, 3008.
(65) Clemmer, D. E.; Sunderlin, L. S.; Armentrout, P. B. *J. Phys. Chem.* **1990**, *94*, 208.

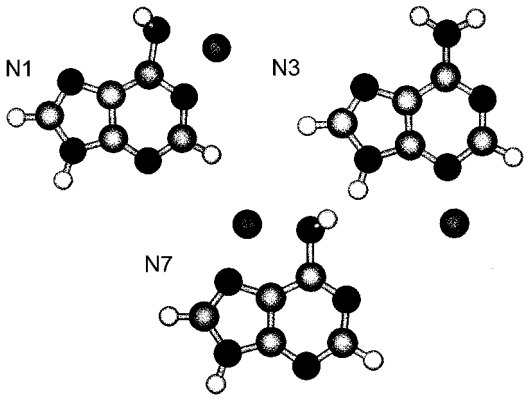

Figure 3. Stable geometries of Cu^+(adenine) complexes bound at the N1, N3, and N7 sites, optimized at the B3LYP/6-31G* level of theory.

with the amino group. In the neutral adenine molecule, the NH_2 group is nearly planar and almost sp^2-hybridized to allow delocalization of the lone pair electrons with the aromatic π-electrons of the purine rings. (The C6−NH_2 bond order of free adenine is generally regarded as 1.51−1.47.)[67] Upon metal ion complexation at the N7 site, chelation with the amino group requires that it rotate out of the plane of the molecule and rehybridize to sp^3. This rehybridization is indicated by the H−N−H bond angle, which changes from 120.4° in neutral adenine to 104.1° in the Cu^+ complex, and by the C6−NH_2 bond length which increases by almost 0.12 Å upon Cu^+ complexation (Table 3S). Our calculations indicate that this rotation and rehybridization of the NH_2 group requires approximately 62 (MP2) − 70 (B3LYP) kJ/mol in the absence of the metal ion. Other than this rotation, the distortion of the adenine molecule that occurs upon complexation to Cu^+ at the N7 site is minor. Bond lengths and angles change in the most extreme cases by less than 0.029 Å and 4.1°, respectively.

When Cu^+ binds at the N3 site, the double bond character of the C6−NH_2 bond is enhanced, as seen by a 0.022 Å decrease in its length. This is consistent with the observation made above that the NH_2 umbrella vibration no longer has a calculated imaginary value. The distortion of the adenine molecule that occurs upon complexation to Cu^+ at the N3 site is again minor. Bond lengths and angles change in the most extreme cases by less than 0.033 Å and 3.1°, respectively. As noted above, binding of the alkali metal ions at the N3 site is less favorable than binding at the N7 chelation site. For Cu^+N3(adenine), theoretical results are very sensitive to the level of electron correlation used. Our MP2 calculations indicate that binding at the N3 site is less stable than at the N7 chelation site by 17.2 kJ/mol, comparable to the differences observed for Li^+ and Na^+, 28.6 and 14.6 kJ/mol, respectively. In contrast, B3LYP calculations find that Cu^+ binds to the N3 and N7 sites with nearly equal affinities, Table 1, even though a chelation interaction is not possible at the N3 site. The MPW1PW91 results are intermediate and indicate that the N7 site is more stable by 4.5 kJ/mol. Clearly, theory does not provide a clear indication of the ground state conformation for Cu^+(adenine), although all three levels of theory agree that the N7 site is favorable.

Binding of Cu^+ at the N1 site is significantly weaker than at the N7 and N3 sites, with comparable BDEs found with B3LYP, MP2, and MPW1PW91 calculations, Table 1. This is somewhat difficult to understand because the N1 site is calculated to have the greatest proton affinity of these three sites, 916.3 kJ/mol at N1 versus 908.0 and 879.3 kJ/mol at N3 and N7, respectively.[4] In addition, its mode of binding is similar to that for the N7 site in that chelation with the amino group occurs, which again requires rotation of the NH_2 group and a concomitant loss of π-resonance delocalization. Calculations here indicate that this rotation and rehybridization requires 64 (MP2) − 71 (B3LYP) kJ/mol, slightly larger than the energy required for distortion of the N7 complex. However, binding at the N1 site forms a four-membered ring rather than a five-membered ring, Figure 3. Sterics of this smaller ring could help explain why the N1 binding site is less favorable than the N3 and N7 sites; however, the alkali cation complexes of adenine bind at the N1 site only slightly less strongly than at the N7 site and the steric considerations should be comparable. An explanation for these differences is offered in the discussion section below.

In the gas phase, we also need to consider the possibility of alternate tautomers to the structure shown in Figure 1, as such tautomers may be accessible in our gas-phase studies even though they are not possible in nucleosides. However, in previous work on the interactions of alkali metal ions with azoles,[27] we demonstrated fairly conclusively that tautomerization of N-heterocycles in the gas phase or upon metal ion complexation did not occur. This was attributed to excessively high potential energy barriers between the possible tautomers.[68] Instead complexation to the most stable gas-phase tautomer of the free ligand was observed exclusively. For the adenine molecule, this is the tautomer identified in Figure 1, N9H, which previous calculations[4] indicate is more stable than the N7H tautomer by 31.0 kJ/mol. Alkali metal ion binding to the N7H tautomer was calculated to be stronger than to N9H by 48−69 kJ/mol. This assumes that tautomerization does not occur upon cleavage of the M^+−adenine bond, an assumption consistent with the results of our previous studies.[27] There were no indications that the experiments could access these M^+(N7H-adenine) complexes, and it seems unlikely that they are formed in the present studies either.

Threshold Analysis. The model of eq 1 was used to analyze the thresholds for reactions 2 in all M^+(adenine) systems except $M^+ = Sc^+$ and Zn^+, reaction 3 for Zn^+(adenine), and reaction 4 in the M^+(adenine) systems for $M^+ = Ti^+$ and V^+. The results of these analyses are provided in Table 2 and a representative analysis is shown in Figure 4 for the Cu^+(adenine) complex. The other systems exhibit comparable results and are shown as Figures 2S in the Supporting Information. In all cases, the experimental cross sections for reactions 2 and 3 are accurately reproduced using a loose PSL TS model.[25] Previous work has shown that this model provides the most accurate assessment of the kinetic shifts for CID processes for electrostatic ion−molecule complexes.[4,14,30,69,70] Good reproduction of the CID data is obtained over energy ranges exceeding 5.5 eV and cross section magnitudes of at least a factor of 100. Table 2 also

(66) Figures were generated using the output of *Gaussian 98* geometry optimizations in Hyperchem Computational Chemistry Software Package, Version 5.0, Hypercube Inc., 1997.
(67) Saenger, W. *Principles of Nucleic Acid Structure*, Springer-Verlag: New York, 1984.
(68) Wong, M. W.; Leung-Toung, R.; Wentrup, C. *J. Am. Chem. Soc.* **1993**, *115*, 2465 and references therein.
(69) More, M. B.; Glendening, E. D.; Ray, D.; Feller, D.; Armentrout, P. B. *J. Phys. Chem.* **1996**, *100*, 1605.
(70) Ray, D.; Feller, D.; More, M. B.; Glendening, E. D.; Armentrout, P. B. *J. Phys. Chem.* **1996**, *100*, 16116.

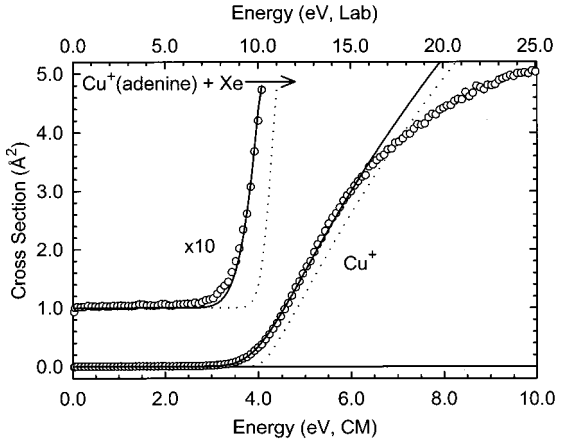

Figure 4. Zero-pressure extrapolated Cu^+ cross section for collision-induced dissociation of the Cu^+(adenine) complex with Xe in the threshold region as a function of kinetic energy in the center-of-mass frame (lower *x*-axis) and the laboratory frame (upper *x*-axis). The solid line shows the best fit to the data using the model of eq 1 including RRKM lifetime effects convoluted over the neutral and ion kinetic and internal energy distributions. The dotted line shows the model cross sections in the absence of experimental kinetic energy broadening for reactants with an internal energy of 0 K.

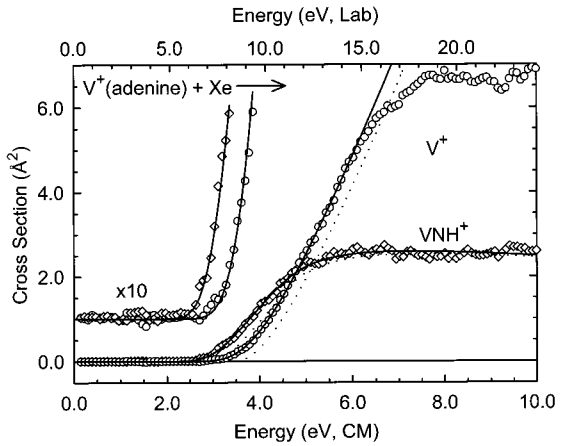

Figure 5. Zero-pressure extrapolated cross sections for interaction of the V^+(adenine) complex with Xe to form V^+ (○) and VNH^+ (◊) in the threshold region as a function of kinetic energy in the center-of-mass frame (lower *x*-axis) and the laboratory frame (upper *x*-axis). The solid lines show the best fits to the data using the model of eq 1 without RRKM lifetime effects convoluted over the neutral and ion kinetic and internal energy distributions. The dotted lines show the model cross sections in the absence of experimental kinetic energy broadening for reactants with an internal energy of 0 K.

includes values of E_0 obtained without including the RRKM lifetime analysis. An example of this kind of fit is shown in Figure 5 for the V^+(adenine) complex. Comparison of these E_0 values with the E_0(PSL) values shows that the kinetic shifts observed for these systems vary from 0.42 to 0.96 eV. The total number of vibrations, 42, and heavy atoms, 11, remains the same in all of the M^+(adenine) complexes and hence the number of low frequency vibrations remains the same. This implies that the observed kinetic shift should directly correlate with the density of states of the complex at threshold, which depends on the measured BDE. This is exactly what is found, as shown in Table 2.

We also considered whether the different frequency sets for Cu^+(adenine) influence the threshold results. We considered cross sections analyzed using frequencies scaled from those calculated for Na^+N7(adenine), those calculated directly for Cu^+N7(adenine), and those calculated directly for Cu^+N3-(adenine). As shown in Table 2, results for these three frequency sets are very similar, with virtually no changes in the analyses without the RRKM analysis and threshold differences of about 0.05 eV for analyses including the kinetic shifts. These differences are well within the 0.08 eV uncertainty associated with the 10% variation in the frequencies and the overall uncertainty of 0.11 eV for any given determination. This properly reflects the fact that these frequencies determine the energy content of the reactant ion and the density of states of the dissociating complex in the RRKM calculations. As long as the number and approximate distribution of the frequencies is reasonably accurate, the results will be relatively insensitive to the exact choices of vibrational frequencies. Coincidentally, the frequencies scaled from Na^+N7(adenine) provide a mean value for the threshold between the frequency sets calculated for the N3 and N7 binding sites. Hence, the use of this scaled frequency set for all metal ions is believed to provide an accurate measure of the true thermodynamic threshold within the listed error bars. We do not evaluate the data using molecular constants calculated for the Cu^+N1(adenine) complex as theory indicates this species is not the ground state conformation.

In the case of the M^+(adenine) systems where $M^+ = Sc^+$, Ti^+, and V^+, competition among reactions 2, 4, 8, and 9 is clearly occurring and certainly influences the threshold determinations. Conservatively the threshold determined for reaction 2 without explicit consideration of this competition is an upper limit to the M^+-adenine BDE. Unfortunately, explicit modeling of the competition requires knowledge of the transition states for reactions 4 and 8, which are likely to be tight transition states. In the absence of accurate transition state information for reactions 4 and 8, we note that the cross sections for reactions 2 and 4 in the vanadium system parallel one another over an extended energy range, Figure 5. Threshold analyses of these two channels (excluding the RRKM analysis of kinetic shifts) indicate relative thresholds separated by 0.5 ± 0.1 eV, Table 2, and are shown in Figure 5.[71] This separation is more than the exothermicity of $V^+ + NH_3 \rightarrow VNH^+ + H_2$, which is 0.12 ± 0.16 eV.[64] This difference reflects the relative energetics of the $NH-H_2$ vs $C_5H_4N_4-NH$ bond energies, i.e., breaking an NH bond of ammonia and forming an H_2 bond vs breaking the C6−N bond of adenine and replacing it with a C6−H bond. In the scandium and titanium systems, the Sc^+-NH and Ti^+-NH bonds are stronger than the V^+-NH bond by 0.87 ± 0.19 and 0.55 ± 0.20 eV,[10,64,65] respectively, such that reaction 4 dominates reaction 2 much more severely, leading to suppression of the latter channel in both systems. In the vanadium system, attempted analysis of the cross section for reaction 8 excluding the RRKM analysis yielded a wide range of threshold values because the cross section rises very slowly. The cross sections for reaction 8 in the scandium and titanium systems can be modeled more easily, but in none of these cases can reliable thermodynamic information be extracted from analyses of these data channels at this time, partly because the structure of the resulting $M^+(C_4H_4N_4)$ product is unknown. However, the availability of transition state parameters and the identification of the product could permit such analyses in the future.

(71) The fit to the cross section for reaction 4 includes a model that approximately accounts for the competition with reaction 2 at higher energies. This model is taken from Weber, M. E.; Elkind, J. L.; Armentrout, P. B. *J. Chem. Phys.* **1986**, *84*, 1521.

The entropy of activation, $\Delta S^{\dagger}$, is a measure of the looseness of the TS and also a reflection of the complexity of the system. It is largely determined by the molecular parameters used to model the energized molecule and the TS, but also depends on the threshold energy. Listed in Table 2, most $\Delta S^{\dagger}$(PSL) values at 1000 K are approximately 70 J K^{-1} mol^{-1} for values determined using the frequencies scaled from Na^+N7(adenine), as expected on the basis of the similarity of these systems. When the calculated Cu^+N7(adenine) frequency set is used, the $\Delta S^{\dagger}$(PSL) drops slightly but is still the same within experimental error; however, when the calculated Cu^+N3(adenine) frequency set is used, the $\Delta S^{\dagger}$(PSL) value drops considerably to about 46 J K^{-1} mol^{-1}. This difference can be understood using the theoretical results. As shown in Figure 3, binding at the N7 chelating site coordinates the amino group, hindering its rotation and stiffening the NH_2 bends as well. Upon dissociation, the motions of the amino group become unhindered and the entropy reflects this change. In contrast, binding at the N3 site is remote from the amino group such that motions of the NH_2 group are largely unaffected upon dissociation. In this regard, the latter $\Delta S^{\dagger}$(PSL) value is comparable to the entropies of activation for a wide variety of noncovalently bound complexes previously measured in our laboratory,[14,17,19,20,24−31] and the $\Delta S^{\dagger}_{1000}$ values in the range of 29−46 J K^{-1} mol^{-1} collected by Lifshitz for several simple bond cleavage dissociations of ions.[72] Likewise the $\Delta S^{\dagger}_{1000}$ value for reaction 3 in the Zn^+ system is lower because the adenine cation has no internal rotor, lowering the entropy of activation.

Conversion from 0 to 298 K. To allow comparison to commonly used experimental conditions, we convert the 0 K bond energies determined here (experimentally and theoretically) to 298 K bond enthalpies and free energies. In the case of the Zn^+(adenine) complex, values for both the Zn + adenine$^+$ product asymptote directly measured experimentally and the Zn^+ + adenine product asymptote are provided. The latter is calculated from the former using the ionization energies of Zn, 9.39405 ± 0.00006 eV,[60] and the vertical ionization energy for adenine, 8.46 ± 0.05 eV, that is the average of two similar values from the literature: 8.44 ± 0.03[61] and 8.48 eV.[62,63] The resulting Zn^+−adenine 0 K bond energy of 2.47 ± 0.07 eV is a lower limit to the true value, which should be higher by the difference in the adiabatic and vertical IE values of adenine. However, the onset in the photoelectron spectrum of adenine is fairly sharp,[63] indicating that this difference is less than a couple tenths of an electronvolt.

The enthalpy and entropy conversions of Table 3 are calculated using standard formulas (assuming harmonic oscillator and rigid rotor models) and the vibrational and rotational constants described therein. Table 3 lists 0 and 298 K enthalpy, free energy, and enthalpic and entropic corrections for all systems experimentally determined (from Table 2). Uncertainties in the enthalpic and entropic corrections are determined by 10% variation in the molecular constants. For the metal systems, where the metal−ligand frequencies are very low and may not be adequately described by theory, the listed uncertainties also include changing the three metal−ligand frequencies by a factor of 2. The latter provides a conservative estimate of the computational errors in these low-frequency modes and is the dominant source of the uncertainties listed. Uncertainties in the corrections used for the experimental values also include the dispersion associated with using molecular constants calculated using B3LYP theory.

(72) Lifshitz, C. *Adv. Mass Spectrom.* **1989**, *11*, 113.

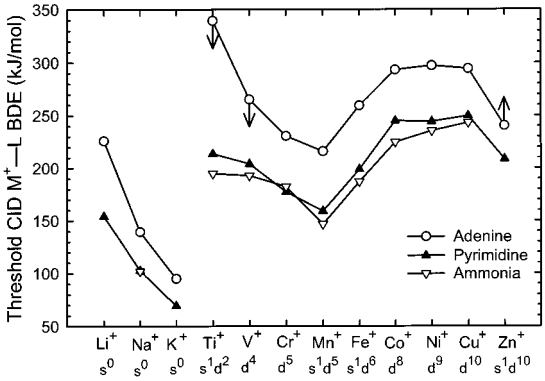

Figure 6. Periodic trends in experimental bond dissociation energies (in kJ/mol) for M^+−L where L = adenine (○), pyrimidine (▲), and ammonia (▽). All values are at 0 K and are taken from Table 3, Amunugama and Rodgers,[18,20] and Walter and Armentrout,[15] respectively.

Discussion

Comparison with Ammonia and Pyrimidine. Figure 6 compares the present experimental results to those obtained in earlier studies for the binding of the transition metal ions to pyrimidine[19] (a model of the N3 and N1, and to a lesser extent, the N7 sites in adenine) and ammonia[15] (similar to the amino group). The most obvious conclusion that can be drawn from this figure is that adenine is bound more strongly than the smaller ligands but that the trends are similar. Simplistically, this is the result expected on the basis of the polarizabilities of these systems (13.1 Å^3 for adenine[23] vs 8.61 Å^3 for pyrimidine[73] vs 2.16 Å^3 for ammonia[74]) and the dipole moments (2.54,[4] 2.31,[75] and 1.47 D,[74] respectively). We find that the adenine BDEs are 25 ± 7% larger than the pyrimidine BDEs, between the 52% increase in polarizability and the 10% increase in dipole moment. However, the adenine BDEs are only 33 ± 9% larger than the ammonia BDEs, even though the polarizability of adenine is 6 times larger than that of ammonia and the dipole moment is 73% larger. Thus, the bond energies are not linearly dependent on the polarizabilities or dipole moments, indicating that the bond lengths probably vary and that other factors, such as chelation and adenine conformation, are influential.

A more precise comparison of the relative adenine vs pyrimidine or ammonia BDEs shows that these systematically decrease across the periodic table. Specifically, V^+, Cr^+, Mn^+, and Fe^+ bind to adenine by 32 ± 3% more than to pyrimidine and 38 ± 8% more than to ammonia. In contrast, for Co^+, Ni^+, Cu^+, and Zn^+, the increases for adenine are 19 ± 3% compared to pyrimidine and 26 ± 5% compared to ammonia. Because the early metal ions have empty 3d orbitals, they can strengthen metal−ligand bonds by accepting π-electron density, whereas late metal ions cannot do this as effectively because the acceptor orbitals are partially occupied.[15] Thus, these relative periodic trends suggest that adenine is a better π-donor than ammonia, generally considered to be a nearly pure σ-donor, or pyrimidine, which also has been shown to be primarily a σ-donor, but also

(73) Miller, K. J. *J. Am. Chem. Soc.* **1990**, *112*, 8533.
(74) Rothe, E. W.; Bernstein, R. B. *J. Chem. Phys.* **1959**, *31*, 1619.
(75) Boulton, A. J.; McKillop, A. *Comprehensive Heterocyclic Chemistry*; Katritzky, A. R., Rees, C. W.; Eds.; Pergamon Press: Oxford, 1984; Vol. 2, p 7.

a weak π-donor. Indeed, comparison of the BDEs between the metal ions and adenine versus those to H_2O, which is a both a σ-donor and a weak π-donor[9] (but stronger than pyrimidine)[19] shows very similar trends across the periodic table, i.e., a relatively uniform 83 ± 11% enhancement for V^+ through Cu^+.

Another interesting comparison that may provide insight into the chelation geometry is to a bis-ligated system, $M^+(NH_3)_2$.[15] Here we find a relatively uniform change in relative bond energies, i.e., M^+(adenine) bond energies are 65 ± 7% of the sum of the bonds in the corresponding $M^+(NH_3)_2$ complexes (with early metals at the high end of this range and late metals at the low end). This relatively uniform increase may be some indication that chelation is involved in the adenine structures, but it also shows that this chelation is not nearly as strong as two independent ligands. As in previous work,[6−8,22,70] this is true when there are geometric restrictions imposed by the chelating ligand, but for adenine there is also a loss of π-resonance delocalization upon chelation. Indeed, addition of an estimate for the lost π-resonance delocalization (see below) to the M^+(adenine) BDEs brings these values to 82 ± 8% of the corresponding $M^+(NH_3)_2$ complexes (again with early metals at the high end of this range and late metals at the low end). This π-resonance delocalization and the geometric restrictions associated with the chelation interactions are explored in more detail in the following sections.

As noted above, the V^+(adenine) BDE limit is stronger than the BDEs for $V^+(NH_3)$ and V^+(pyrimidine) by an amount that is comparable to the increases observed for the analogous complexes of Cr^+, Mn^+, and Fe^+. This observation gives us some confidence that the V^+(adenine) limit cited in Tables 2 and 3 is close to the true thermodynamic bond energy. In contrast, the upper limit for the Ti^+(adenine) BDE is 59% and 74% greater than the BDEs of Ti^+ to pyrimidine and ammonia, respectively. Because these relative BDEs are so much larger than for the other first row transition metal ions, it likely that the upper limit for the Ti^+(adenine) BDE is well above the true thermodynamic value. Hence, this value was excluded from the discussion of the trends above.

Periodic Trends in the Binding of Metal Ions to Adenine. Noncovalent bonds to metal monocations are controlled by a balance between ion-induced dipole and ion−dipole attractions and Pauli repulsion between the metal ion and the ligand. For transition metals, the ionic radius decreases from left to right across the periodic table, such that the electrostatic contribution to bonding should increase. Therefore, the late transition metal ions generally bind more strongly than the early metal ions, as can be seen in Figure 6. This figure also makes it clear that the first row transition metal ions bind much more strongly to any of the donors than does K^+, the $4s^0$ ion of the same periodic row. Clearly, changes in the d orbital occupation play a significant role in the bonding energetics. The strong variations in the binding among the first row transition metals have previously been explained for other metal−ligand complexes by characterizing several mechanisms by which a transition metal ion is capable of decreasing Pauli repulsion between the metal and the ligand.[13,15,16,19,76−78]

For the transition metals considered here, these mechanisms include 4s−3dσ hybridization and promotion to a more favorable electronic state. 4s−3dσ hybridization moves electron density away from the ligand, placing it in a direction perpendicular to the bonding axis, thereby increasing the effective nuclear charge.[15,19,20,79,80] Such hybridization involves a transition metal center existing in a state that is a combination of low-spin $4s^13d^n$ and $3d^{n+1}$ configurations. Promotion to an electronically excited state is a second mechanism by which Pauli repulsion can be reduced. The thermodynamic consequences of changing spin state to optimize metal−ligand bonding have been observed in the cases of manganese and iron, where the high-spin $^7S(4s^13d^5)$ and $^6D(4s^13d^6)$ ground states cannot engage in 4s−3dσ hybridization because there are no high-spin $3d^6$ or $3d^7$ states possible. In these cases, it is necessary to promote to a state of lower spin (a quintet for Mn^+ and a quartet for Fe^+) before 4s−3dσ hybridization can occur.

In discussing the details of the present bond energies, it is easiest to start with the Co^+, Ni^+, and Cu^+ ions, which have ground-state electron configurations of $3d^n$ (n = 8, 9, and 10, respectively). This allows for direct σ-donation of an electron pair of the ligand into the empty 4s orbital of the metal ion. Although the 3dσ orbital is occupied in these systems, the size of these metal ions is smaller than for earlier metal ions and 4s−3dσ hybridization mediates the repulsive effects of this occupation, such that the bond strengths of the late metals are strong.

Interaction of ligands with iron is weaker than the other late metals because the ground state of Fe^+ is $^6D(4s^13d^6)$, such that the 4s orbital is not empty. However, Fe^+ has a ^4F excited state that lies only 22.4 kJ/mol above the ^6D ground state.[81] The excited state has an $3d^7$ configuration that should decrease the Pauli repulsion between the metal ion and the adenine ligand and can utilize 4s−3dσ hybridization. The Fe^+ bond energy is 34 ± 14 kJ/mol weaker than the Co^+ bond energy, slightly larger than the relative bond energies observed for analogous ammonia[15] and pyrimidine[20] complexes. The weaker bond of Fe^+-(adenine) relative to Co^+(adenine) is consistent with a quartet ground state that dissociates adiabatically to $Fe^+(^6D)$, 22 kJ/mol lower than the diabatic asymptote. It is also possible that the weaker bond energy could correspond to a sextet ground state that is weaker because of the 4s orbital occupation, but then we would anticipate a bond energy closer to that of Mn^+, which is much weaker than that of Fe^+ (Table 2).

For Mn^+ and Zn^+, the ground-state configurations have occupied 4s orbitals, $^7S(4s^13d^5)$ and $^2S(4s^13d^{10})$, respectively, which lead to more repulsive interactions with the ligand. Unlike Fe^+, there is no low-lying electronic state having a $3d^n$ configuration, so that the weak Mn^+−adenine and Zn^+−adenine bonds reflect the unfavorable occupation of the 4s orbital. Zn^+ binds more strongly than Mn^+ because the former ion is smaller. It is possible that these metal ions may minimize Pauli repulsion by utilizing s−p hybridization, which polarizes electron density 180° away from the bonding axis, thereby increasing the effective nuclear charge. However, the energetic cost of such hybridization is greater than for s−dσ hybridization for other metal ions.[15]

V^+ and Cr^+ have high-spin ground states, $^5D(3d^4)$ and $^6S(3d^5)$, with unoccupied 4s orbitals. These metal ions form

(76) Rosi, M.; Bauschlicher, C. W. *J. Chem. Phys.* **1989**, *90*, 7264.
(77) Rosi, M.; Bauschlicher, C. W. *J. Chem. Phys.* **1990**, *92*, 1876.
(78) Armentrout, P. B. *Acc. Chem. Res.* **1995**, *28*, 430.
(79) Bauschlicher, C. W.; Langhoff, S. R.; Partridge, H. *J. Chem. Phys.* **1991**, *94*, 2068.
(80) Koizumi, H.; Zhang, X.-G.; Armentrout, P. B. *J. Phys Chem. A* **2001**, *105*, 2444.
(81) Sugar, J.; Corliss, C. *J. Phys. Chem. Ref. Data* **1985**, *14*, Suppl. 2, p 1.

weaker bonds than those of the late metal ions largely because the radii of the early metal ions are larger, leading to longer bonds. The bond for V^+ is stronger than that for Cr^+ because the 3dσ orbital can be left empty for the former metal ion, thereby keeping Pauli repulsion with the adenine ligand to a minimum. The upper limit obtained for the Ti^+−adenine bond energy is much higher than that for V^+, but comparison with other ligands in the previous section suggests that this limit is probably not close to the true thermodynamic value.

In addition to these trends, which focus on the σ-acceptor properties of the metal ions, the metal ions can also accept (or donate) π-electron density. This is most easily ascertained by comparison to other ligands, as discussed in the previous section. There the periodic trends (comparison of early vs late metal ions) indicate that adenine is a π-donating molecule. This enhances the bonds to early metal ions, which can have empty π-accepting orbitals, relative to the late metal ions.

Comparison of Theory and Experiment. Table 1 lists the 0 K binding energies for the alkali metal cations and Cu^+ calculated at the B3LYP/6-311+G(2d,2p)//B3LYP/6-31G* level, the MP2(full)/6-311+G(2d,2p)//B3LYP/6-31G* level, the MPW1PW91/6-311+G(2d,2p)// MPW1PW91/6-31G* level, and B3LYP single point calculations that include 3df polarization functions on the metals. This augmented polarization set enhances the calculated bond energies by less than 2 kJ/mol in all cases (an average difference of 1.0 ± 0.6 kJ/mol). Table 1 also includes the latter values and MP2 bond energies including ZPE and BSSE corrections.[82−84] For the alkali metal cations, the MP2 values listed were previously calculated at the MP2(full)/6-311+G(2d,2p)//MP2(full)/6-31G* level including ZPE and BSSE corrections.[4] The B3LYP and MP2 values are in reasonable agreement with one another with a mean absolute deviation (MAD) of 4.4 ± 1.6 kJ/mol, except for the Cu^+N3(adenine) values which disagree by 14.1 kJ/mol. The MPW1PW91 calculations are essentially intermediate, having a MAD of 3.5 ± 2.4 kJ/mol with the B3LYP results and 3.9 ± 3.3 kJ/mol with the MP2 results. All theory numbers are lower than experiment. Indeed, the B3LYP values for all four metal ions are 13 ± 8% lower than the experimental values with a MAD between experiment and theory of 19.4 ± 9.4 kJ/mol. Agreement between experiment and the MP2 and MPW1PW91 calculations is comparable, with MADs of 19.2 ± 8.7 and 22.6 ± 8.9 kJ/mol, respectively. For all three types of calculations, the MADs are larger than the average experimental error.

Previously,[4] we have hypothesized that theory may systematically underestimate the bond energies for adenine complexes because of the difficulties in describing the π-resonance delocalization and because of covalency in the metal−ligand bond. The covalency, which roughly increases as the bond strength increases, can be estimated on the basis of the charge retained on the metal ion in the complexes (as taken from MP2 calculations): ~0.76e on Li^+, ~0.90e on Na^+, ~0.98e on K^+,[4] ~0.65e on Cu^+(N7), ~0.72e on Cu^+(N3), and ~0.51e on Cu^+(N1). Although these results clearly indicate that the bonding is largely electrostatic, especially for Na^+ and K^+, there are clear indications of covalency in the metal−ligand bonds for the Li^+ and Cu^+ systems. As noted previously,[4] this may mean that the level of theory used here may be inadequate for a complete description of these systems. However, it is also possible that this additional covalency means that the TSs for dissociation of the Li^+ and Cu^+ complexes are not adequately described by the PSL model. If the transition states were tighter in these cases, then the kinetic shifts would be larger and the thresholds measured smaller, in better agreement with theory. However, theory and experiment also do not agree for the Na^+ and K^+ complexes. For these species, the kinetic shifts are much smaller and the metal−ligand bonds more electrostatic, such that the PSL treatment is almost certainly appropriate and the results would not change greatly with different assumptions about the TS.

Adenine Binding Site for Transition Metal Ions. The most stable conformations of the Cu^+N7(adenine) and Cu^+N1(adenine) complexes have the amino groups rotated out of the plane, as shown in Figure 3. Thus, the stability of these complexes is partially driven by the chelation interaction. We wish to estimate the thermodynamic consequences of this interaction by calculating the energy gained by chelation, a "chelation energy". In a naive sense, this could be simply the difference between the binding energy to a chelating ligand, such as adenine, and a monodentate analogue, such as imidazole for comparison to the N7 site or pyrimidine to compare to the N1 site. However, we believe a more accurate and useful estimate of the chelation energy defines it as the energy gained in going from metal ion binding to an adenine with the amino group held planar, such as it might be in a DNA duplex, to binding to an adenine that has rotated the amino group to form the strongest possible bond with the metal ion. This requires that we consider three competing effects associated with the interaction of the metal ion with the amino group. Rotation of the amino group out of the plane (i) decreases the stabilization associated with π-resonance delocalization in the free ligand, (ii) decreases repulsion between the metal ion and nearest hydrogen when the amino group is planar, and (iii) enhances binding as a result of interactions between the metal ion and the lone pair of electrons on the amino group. In essence, our chelation energy is a measure of how the latter two energies overcome the distortion of π-resonance delocalization.

The first effect, π-resonance delocalization, is expected to have only a modest dependence upon the metal ion. We estimate this effect as the difference in energies of free adenine in its most stable conformation (planar) and that of free adenine in the distorted geometry of the Cu^+N7(adenine) complex. The MP2 calculations indicate that this distortion costs about 62 kJ/mol, whereas both DFT calculations find 70 kJ/mol. Both values are somewhat larger than the values calculated at the MP2 level for the three alkali metal ions, 59 kJ/mol for Li^+, and 55 kJ/mol for both Na^+ and K^+.[4] Nuclear magnetic resonance studies indicate that a similar distortion for cytosine costs 63−75 kJ/mol and less for adenine.[67] We estimate the second and third effects by calculating (using the B3LYP/6-311+G(2d,2p)//B3LYP/6-31G* level of theory) the binding energy of Cu^+ at the N7 site of adenine with the geometry of the ligand fixed to that of the free base, but the Cu^+ free to adjust its position. In this configuration, the Cu^+ ion remains in the plane of the molecule, but adjusts its position to maximize bonding to the imidazolic nitrogen atom, N7, and minimize the repulsive interaction with the nearest H atom of the amino group.

(82) Møller, C.; Plesset, M. S. *Phys. Rev.* **1934**, *46*, 618.
(83) Bartlett, R. J. *Annu. Rev. Phys. Chem.* **1981**, *32*, 359.
(84) Hehre, W. J.; Radom, L.; Schleyer, P. v. R.; Pople, J. A. *Ab Initio Molecular Orbital Theory*, Wiley: New York, 1986.

Compared to the fully optimized, chelating Cu^+N7(adenine) complex, the Cu−N7 bond length is 1.783 Å, 0.107 Å shorter, the Cu−NH_2 distance is 3.190 Å, 1.23 Å longer, and the CuN7C5 bond angle opens up to 126.7°, 34.0° larger. This constrained complex is less stable than the chelating Cu^+N7-(adenine) complex by 36 kJ/mol, comparable to values determined previously for Li^+, Na^+, and K^+, of 62, 44, and 27 kJ/mol, respectively. These differences are relatively low because the H-atom repulsion is partially compensated by enhanced binding at the N7 site (indicated by the shorter bond length). Our final chelating energy comes from combining these two B3LYP results, as this represents the binding energy gained upon rotation of the amino group to chelate combined with the π-resonance delocalization energy overcome in accomplishing this rotation. This provides an estimate for the chelation energy of ~106 kJ/mol. Using this same procedure for Li^+, Na^+, and K^+, we estimate the chelation energy of the N7 complex to these ions as 117, 99, and 82 kJ/mol, respectively. These values are about 10% smaller than earlier estimates of the chelation energy made for these alkali metal ions of 129, 110, and 90 kJ/mol,[4] respectively. The latter values were determined based on a slightly differing definition of the chelation energy, which accounts for the slightly different values obtained by the present procedures. The fact that similar values are obtained suggests that the estimates are reasonably robust. An explicit calculation of the chelation energy for the N1 conformer was not performed as this complex does not appear to be important experimentally.

Although theory is inconclusive with regard to the relative binding energies of Cu^+ at the N7 and N3 sites of adenine, they agree that the N1 site is the least favorable site by over 18 kJ/mol relative to the ground state conformation. This contrasts with the alkali metal cations where the two sites that can chelate with the amino group, N7 and N1, have comparably strong BDEs and binding at N3 is weaker. One reason that binding at the N3 site can compete favorably with the N7 site is that the former does not require rotation of the NH_2 group, avoiding the loss of resonance delocalization that costs about 62−70 kJ/mol. In addition, the Cu^+−N bond length is 0.113 Å shorter in the N3 complex than in the N7 complex, partially compensating for the lack of a chelation interaction. However, both of these circumstances are also true for alkali cation complexes where binding at the N7 site is still favored. One difference between the binding of the alkali ions and Cu^+ at the N3 site can be summarized by the M^+−N3−C4 bond angle: 127.3° for Cu^+, 137.7° for Li^+, 141.3° for Na^+, and 146.4° for K^+. In these systems, the metal ion is pushed away from the optimal angle of 124.4° by a repulsive interaction with the hydrogen atom on N9.[85] However, because this angle is smallest for Cu^+, the overlap with the pair of electrons on N3 is presumably highest for this metal, allowing a stronger bond that helps overcome the lack of a chelating interaction. In addition, whereas adenine binds to Cu^+ as a monodentate ligand at the N3 site, the N7 site is bidentate chelating. In the former case, 4s−3dσ hybridization can be completely effective in enhancing the bonding, whereas it is known that for two ligands, 4s−3dσ hybridization prefers a geometry in which the two ligands are located 180° from one another, i.e., a linear L−M-L arrangement.[15,21,80] Because of the constraints of the adenine rings, the N−Cu−NH_2 bond angle cannot approach 180° for either the N7 or N1 sites. Indeed, we calculate this angle is only 102.3° for the Cu^+N7(adenine) complex, and only 72.6° in the N1 complex. Consequently, 4s−3dσ hybridization is not as effective for the chelating sites as for the N3 site. Further, it is less effective for N1 compared to N7, explaining why the N1 site is less favorable for Cu^+ than observed for the alkali metal cations. In contrast, the smaller alkali metal cations, which are spherically symmetric even when ligated, benefit from chelation at any angle. Larger alkali metal cations, starting about K^+, along with Mn^+ and Zn^+ can utilize s−p hybridization to reduce Pauli repulsion, but this hybridization allows chelating angles close to 90°, which is useful for the adenine ligand. This would serve to enhance the chelation interaction of these metal ions with adenine relative to that observed for other metal ions which do not make use of s−p hybridization. The present results are inconclusive in this regard, however, because examination of the BDEs to adenine relative to those measured for pyrimidine indicates no enhancement for K^+ and a small enhancement for Mn^+. Zn^+ shows a depression; however, this comparison may not be meaningful because the value measured for Zn^+(adenine) is a lower limit to the true BDE.

(85) Even in its uncomplexed geometry, the six-membered ring is distorted such that the C4−N3−C2 bond angle is calculated to be 111.1°. Hence, symmetric binding to the lone pair of electrons on N3 requires a C4−N3−M bond angle of approximately 124.4° = (360.0° − 111.1°)/2.

Conclusions

The kinetic energy dependences of the collision-induced dissociation of M^+(adenine), where $M^+ = Sc^+$, Ti^+, V^+, Cr^+, Mn^+, Fe^+, Co^+, Ni^+, Cu^+, and Zn^+ with Xe are examined in a guided ion beam mass spectrometer. The dominant dissociation process in most cases is loss of the intact adenine ligand, although the Sc^+, Ti^+, and V^+ complexes show extensive bond activation processes that compete with this channel. Thresholds for the simple CID processes are determined after consideration of the effects of reactant kinetic and internal energy distributions, multiple collisions with Xe, and lifetime effects (using methodology described in detail elsewhere).[25] Insight into the structures and binding of the metal ions to the adenine molecules is provided by theoretical calculations of the Cu^+ complex performed at the B3LYP/6-311+G(2d,2p)//B3LYP/6-31G*, MP2(full)/6-311+G(2d,2p)//B3LYP/6-31G*, and MPW1PW91/6-311+G(2d,2p)//MPW1PW91/6-31G* levels of theory. All three levels of theory agree that the N7 binding site is favorable and that N1 is substantially weaker, but theory disagrees about the relative stability of the N3 binding site. B3LYP finds the N3 site comparable to N7 for Cu^+, whereas MPW1PW91 and MP2 find the N7 site is favored by 5 and 17 kJ/mol, respectively. In any event, these results are in contrast to the alkali metal cations where N1 and N7 are comparably strong binding sites, and N3 is weaker. This difference in relative binding affinities is explained using 4s−3dσ hybridization, which may enhance the binding at N3 more than at N7 because of the preferred 180° directionality of bidentate binding to 4s−3dσ hybrids. Binding at the N7 chelation site is stronger than that at N1 chelation site for the same reason.

An interesting consequence of these results is predictions for metal-induced stability changes in DNA duplexes. Specifically, we previously noted that binding of alkali metal cations to adenine, which occurs preferentially at the N7/NH_2 chelation site, would tend to disrupt the hydrogen bonding of A:T pairs.[4] This is equally true of the transition metal ions when binding occurs at the N7/NH_2 chelation site. However, disruption of a

single H-bond in an AT base pair costs about 27 kJ/mol,[86] more than the calculated difference in binding affinities of the N3 and N7 sites. Thus, late transition metal ions may preferentially bind at N3, such that H-bonding between bases is not disrupted. In fact, binding at the N3 site should cause the amino H atoms to become more acidic, which should result in an enhancement of the hydrogen bonding in duplex DNA. However, early transition metals, such as Sc^+, Ti^+, and V^+, may bind and activate covalent bonds in the nucleic acids, leading to damage of the DNA. Similar destructive behavior might also be expected for any transition metal ion (such as a multiply charged species) that is not adequately solvated to reduce its reactivity.

(86) The interaction energy of the hydrogen bonding in an A:T pair as measured for isolated bases methylated at the glycosidic bond is about 54 kJ/mol (Yanson, I.; Teplitsky, A.; Sukhodub, L. *Biopolymers* **1979**, *18*, 1149).

Acknowledgment. This work was supported by the National Science Foundation, Grant CHE-9877162, and in part by an ASMS Research Award from Micromass (M.T.R.). Early parts of this work were supported by the Petroleum Research Fund, administered by the American Chemical Society.

Supporting Information Available: Tables of vibrational frequencies and average vibrational energies, rotational constants, and B3LYP/6-31G* and MPW1PW91/6-31G* geometry optimized structures of adenine, adenine$^+$, and M^+(adenine) complexes ($M^+ = Li^+$, Na^+, K^+, and Cu^+). Figures showing cross sections for the collision-induced dissociation of M^+-(adenine) complexes (PDF). This material is available free of charge via the Internet at http://pubs.acs.org.

JA011278+